Isotope effects in the lattice structure and vibrational and optical spectra of ${}^6Li_x{}^7Li_{1-x}YF_4$:Ho crystals

N. I. Agladze and M. N. Popova

Institute of Spectroscopy, Russian Academy of Sciences, 142092 Troitsk, Moscow Oblast, Russia

M. A. Koreĭba, B. Z. Malkin, and V. R. Pekurovskiĭ

Kazan State University, 420008 Kazan, Russia

(Submitted 29 June 1993)
Zh. Eksp. Teor. Fiz. **104**, 4171–4193 (December 1993)

High-precision measurements of the optical absorption spectra of impurity holmium ions in $LiYF_4$ crystals with different isotopic compositions in the lithium are carried out. The changes of the vibrational spectrum, lattice structure, and crystal-field parameters in ${}^6LiHoF_4$ crystals in comparison with ${}^7LiHoF_4$ crystals are calculated, as are the local lattice deformation and the corresponding changes of the crystal field acting on the Ho^{3+} ions near isolated impurity ions of ${}^6Li$ (${}^7Li$) in the ${}^7LiYF_4$ (${}^6LiYF_4$) lattice. The results of the calculations are used to interpret the experimental data on the optical spectra of ${}^6Li_x{}^7Li_{1-x}YF_4$:Ho(0.1%) crystals.

INTRODUCTION

In this paper we present the results of high-precision measurements of the hyperfine structure in the optical absorption spectrum of holmium impurity ions in $LiYF_4$ crystals with different isotopic compositions in the lithium sublattice, and calculate the isotopic structure of the spectra that arises from a random distribution of ${}^6Li$ and ${}^7Li$ isotopes with the natural contents 7.42% and 92.58%, respectively (preliminary results and a qualitative interpretation of the experimental data are given in Ref. 1). Isotopic disorder in a crystal lattice can be manifested in the energy spectrum of impurity ions as a consequence of the inhomogeneity of the crystal field and the dynamical characteristics of the lattice. The previously studied isotopic effects in the optical spectra of activated crystals are due to the difference in the masses of the nuclei of the emitting (or absorbing) ions: MgO, Al_2O_3:Cr^{3+} (Refs. 2, 3), ZnS:Cu^{2+},Ni^{2+} (Ref. 4), $LaCl_3$:Nd^{3+} (Ref. 5), Ni^+ in diamond; the isotope shift of the zero-phonon lines has been interpreted as the result of the interaction of optical electrons with locally perturbed lattice vibrations that depend on the mass of the impurity ion, and local static changes of the lattice structure near the different isotopes have not been taken into account. Spectral effects resulting from isotopic disorder in a lattice have been observed in infrared absorption induced by impurity ions in KI:Ag^+ crystals with the natural 7% content of the isotope ${}^{41}K$ (Ref. 7); isotope shifts of the zero-phonon lines and phonon wings in the spectra of optical centers in diamond activated by the isotopes ${}^6Li$ and ${}^7Li$ have been investigated in Refs. 8 and 9.

In recent years a careful study has been made of the dependence of the structure constants of a number of simple compounds (of germanium[10] and diamond[11]) on isotopic composition, this dependence being a consequence of anharmonic interactions between atoms in the crystal. In particular, when ${}^{12}C$ is replaced by ${}^{13}C$ the lattice constant a of diamond at room temperature decreases by 5.5×10^{-4} Å (the relative change $\Delta a/a$ of the interatomic spacings, divided by the relative change $\Delta m/m$ of the mass, is equal to 1.855×10^{-3}; see Ref. 11). The relative change of the mass of the isotopes ${}^6Li$ and ${}^7Li$ is 16.7%, and, for ${}^6Li_x{}^7Li_{1-x}YF_4$ crystals, upon change of the concentration of the isotope ${}^6Li$ from 0 to 1, we may expect changes of the structure constants of the order of $3\times10^{-2}\%$. The crystal-field parameters in this case change by approximately 0.1%, and, since the Stark splittings of the rare-earth-ion multiplets amount to 100 cm^{-1} in order of magnitude, the shifts of the spectral lines of the impurity rare-earth ions with change of the relative content of the isotopes of lithium in $LiYF_4$ crystals can amount to approximately 0.1 cm^{-1}. This rough estimate is in agreement with the results of measurements.

The aim of the present work was to develop a quantitative theory of isotope spectral effects on the basis of semi-phenomenological models of the crystal field, lattice dynamics, and electron–phonon interaction in rare-earth insulators—in particular, the models used previously in the description of the magnetoelastic properties of the lithium–rare-earth double fluorides.[12] With the aim of simplifying the calculations and displaying the basic mechanisms of the effect of isotopic disorder in the matrix on the spectra of the impurity ions, we have not taken into account the change of the structure and dynamical characteristics of the $LiYF_4$:Ho lattice near the impurity holmium ions that substitute for yttrium ions. In fact, we have calculated the changes of the vibrational spectrum and the structure parameters and crystal-field parameters in regular $LiHoF_4$ crystals upon substitution of the isotope ${}^7Li$ by the isotope ${}^6Li$ in the lithium sublattices, and also the local deformation of the lattice and the corresponding changes of the crystal field acting on the Ho^{3+} ions near isolated ${}^6Li^+$ (${}^7Li^+$) impurity ions in the ${}^7LiHoF_4$ (${}^6LiHoF_4$) lattice. Since the Y^{3+} and Ho^{3+} ions are of almost the same size, and the vibrational spectra of $LiYF_4$ and $LiHoF_4$ crystals

1063-7761/93/121021-13$10.00

differ only slightly,[13–15] we assume that it is possible to use the results of the calculations to interpret the data from investigations of the spectra of $^6\mathrm{Li}_x{}^7\mathrm{Li}_{1-x}\mathrm{YF}_4$:Ho crystals, in which the impurity holmium ions play the role of optical probes of isotope effects in the structure of the matrix.

1. STRUCTURE CONSTANTS AND VIBRATIONAL SPECTRA OF ^{6}LIHoF$_4$ AND ^{7}LIHoF$_4$ CRYSTALS

The potential energy of a crystal lattice does not depend on the masses of the atoms constituting it. In the framework of the harmonic approximation a change of isotopic composition leads only to changes of the dynamical characteristics of the lattice—in particular, the vibrational frequencies and the mean-square displacements of the atoms from their equilibrium positions. The spacings between the atoms, as in thermal expansion, change only as a consequence of anharmonicity of the lattice vibrations.

We represent the potential energy of a lattice with a basis (k labels the sublattice) in the form of a series in the static ($\mathbf{u}$) and dynamic (ξ) displacements of the constituent atoms from their equilibrium positions (we use a matrix form for writing convolutions over the coordinates and labels of the atoms):

$$\Phi=\Phi_0+\frac{1}{2!}\,\Phi''(\mathbf{u}+\zeta)^2+\frac{1}{3!}\,\Phi'''(\mathbf{u}+\xi)^3+\dots. \tag{1}$$

In the case of uniform deformation the static displacements are equal to

$$u_\alpha\begin{pmatrix}L\\k\end{pmatrix}=e_{\alpha\beta}X_\beta\begin{pmatrix}L\\k\end{pmatrix}+w_\alpha(k), \tag{2}$$

where L is the cell label, $e_{\alpha\beta}$ are the components of the strain tensor, $\mathbf{X}(^L_k)$ are the lattice-site vectors, and $\mathbf{w}(k)$ is the vector describing the displacement of the kth sublattice (here and below, repeated Greek indices are summed over). When the first nonzero term due to anharmonicity of the interatomic interactions is taken into account the corresponding change of the free energy of the lattice takes the form

$$F=\tfrac{1}{2}\Phi''(\mathbf{eX}+\mathbf{w})^2+\tfrac{1}{2}\Phi'''(\mathbf{e}X+\mathbf{w})\langle\xi\xi\rangle, \tag{3}$$

where the angular brackets $\langle\dots\rangle$ denote averaging over the canonical ensemble of the harmonic lattice. We expand the dynamic displacements (which satisfy the equations of motion $m\ddot{\xi}=-\nabla_\xi\Phi$) in normal coordinates $Q(f)$ of the lattice, which contains N cells:

$$\xi_\alpha\begin{pmatrix}L\\k\end{pmatrix}=\frac{1}{\sqrt{N}}\sum_f a_\alpha\left(\begin{matrix}L\\k\end{matrix}\middle|f\right)Q(f). \tag{4}$$

For a regular lattice the diagonal matrix $\mathbf{m}$ of the atomic masses has elements $m_{\alpha\beta}(^{L}_{k}\ ^{L'}_{k'})=m_k\delta_{\alpha\beta}\delta_{LL'}\delta_{kk'}$; in this case, $f=(\mathbf{q}j)$, where $\mathbf{q}$ is the phonon wave vector and j labels the branch of the vibrational spectrum; the coefficients of the expansion (4) are equal to

$$a_\alpha\left(\begin{matrix}L\\k\end{matrix}\middle|f\right)=\frac{1}{\sqrt{m_k}}\,e_\alpha\left(k\middle|\begin{matrix}q\\j\end{matrix}\right)\exp\left(i\mathbf{q}\mathbf{X}\begin{pmatrix}L\\k\end{pmatrix}\right), \tag{5}$$

where $e_\alpha(k|^q_j)$ are the components of the polarization vector of the vibrational mode with frequency $\omega_j(q)$ and are eigenvectors of the lattice dynamical matrix

$$D_{\alpha\beta}(kk'|\mathbf{q})=(m_km_{k'})^{-1/2}\sum_L\Phi''_{\alpha\beta}\begin{pmatrix}0&L\\k&k'\end{pmatrix}\times\exp\left(i\mathbf{q}\mathbf{X}\begin{pmatrix}L&0\\k'&k\end{pmatrix}\right). \tag{6}$$

Here, $\mathbf{X}(^L_{k'}\ ^O_k)=\mathbf{X}(^L_{k'})-\mathbf{X}(^O_k)$ and $\Phi''_{\alpha\beta}(^O_k\ ^L_{k'})=\partial^2\Phi/\partial u_\alpha(^O_k)\partial u_\beta(^L_{k'})$.

The correlation functions $\langle\xi\xi\rangle$ will be expressed in terms of the lattice Green functions $\mathbf{G}=(\mathbf{m}\omega^2-\mathbf{\Phi}'')^{-1}$, which, in the site representation, have elements

$$G_{\alpha\beta}\left(\begin{matrix}L&L'\\k&k'\end{matrix}\middle|\omega\right)=\frac{1}{N}(m_km_{k'})^{-1/2}\times\sum_{\mathbf{q}j}\frac{e_\alpha\left(k\middle|\begin{matrix}q\\j\end{matrix}\right)e^*_{j3}\left(k'\middle|\begin{matrix}q\\j\end{matrix}\right)}{\omega^2-\omega_j(\mathbf{q})^2}\,e^{i\mathbf{qX}(^{L}_{k}\ ^{L'}_{k'})}. \tag{7}$$

Using the equality

$$\langle Q(qj)Q(q'j')\rangle=(2n(\omega_j(q))+1)\times(\hbar/2\omega_j(q))\delta_{jj'}\delta(q+q'), \tag{8}$$

where $n(\omega)$ is the occupation number of the phonons, and going over from summation over the wave vectors to integration, we obtain

$$\left\langle\xi_\alpha\begin{pmatrix}L\\k\end{pmatrix}\xi_\beta\begin{pmatrix}L'\\k'\end{pmatrix}\right\rangle=\frac{\hbar}{2\pi}\int\operatorname{Im}G_{\alpha\beta}\left(\begin{matrix}L&L'\\k&k'\end{matrix}\middle|\omega\right)\times(2n(\omega)+1)\frac{d\omega^2}{\omega}. \tag{9}$$

In accordance with expression (3), we obtain the change of the specific free energy (per cell with volume v_0) upon deformation of the lattice in the form

$$F=\tfrac{1}{2}v_0(\hat{\mathbf{C}}e^2+2\mathbf{bew}+\mathbf{aw}^2)+\mathbf{Te}+\mathbf{Pw}. \tag{10}$$

In the framework of the approximation of pair interactions between the atoms constituting the lattice, the coefficients in (10) are equal to

$$v_0a_{\alpha\beta}(kk')=(m_km_{k'})^{1/2}D_{\alpha\beta}(kk'|o), \tag{11}$$

$$v_0l_{\alpha\beta,\gamma}(k)=\sum_{Lk'}\Phi''_{\alpha\gamma}\begin{pmatrix}L&0\\k'&k\end{pmatrix}X_\beta\begin{pmatrix}L&0\\k'&k\end{pmatrix}, \tag{12}$$

$$v_0\hat{C}_{\alpha\beta,\gamma\delta}=[\alpha\gamma,\beta\delta]+[\alpha\delta,\beta\gamma]-[\alpha\beta,\gamma\delta], \tag{13}$$

$$[\alpha\beta,\gamma\delta]=-\frac{1}{2}\sum_{Lkk'}\Phi''_{\alpha\beta}\begin{pmatrix}0&L\\k&k'\end{pmatrix}X_\gamma\begin{pmatrix}L&0\\k'&k\end{pmatrix}X_\delta\begin{pmatrix}L&0\\k'&k\end{pmatrix}, \tag{14}$$

TABLE I. Coordinates of ions in the unit cell of the LiYF$_4$ crystal (in units of the lattice constants a,a,c). The structure constants are $a=5.167$ Å, $c=10.73$ Å, $x=0.2820$, $y=0.1642$, $z=0.0815$ (Ref. 16).

Ion	Coordinates			Ion	Coordinates		
F$_1$	y,	$0{,}5-x$,	$0{,}25+z$	F$_5$	y,	$-x$,	$-z$
F$_2$	x,	$0{,}5+y$,	$0{,}25-z$	F$_6$	x,	y,	z
F$_3$	$-x$,	$0{,}5-y$,	$0{,}25-z$	F$_7$	$-x$,	$-y$,	z
F$_4$	$-y$,	$0{,}5+x$,	$0{,}25+z$	F$_8$	$-y$,	x,	$-z$
Li$_1$	0,	0,	0	Y$_1$	0,	0	0,5
Li$_2$	0,	0,5	0,25	Y$_2$	0,	0,5	0,75

$$T_{\alpha\beta}=\frac{1}{2}\sum_{Lkk'}\Phi'''_{\gamma\delta\alpha}\begin{pmatrix}0 & 0 & L\\ k & k & k'\end{pmatrix}X_\beta\begin{pmatrix}L & 0\\ k' & k\end{pmatrix}\left\langle\xi_\gamma\begin{pmatrix}0\\ k\end{pmatrix}\right.$$

$$\left.\times\left(\xi_\delta\begin{pmatrix}0\\ k\end{pmatrix}-\xi_\delta\begin{pmatrix}L\\ k'\end{pmatrix}\right)\right\rangle, \qquad (15)$$

$$P_\gamma(k)=-\frac{1}{2}\sum_{Lk'}\Phi'''_{\alpha\beta\gamma}\begin{pmatrix}L & 0 & 0\\ k' & k & k\end{pmatrix}\left\langle\left(\xi_\alpha\begin{pmatrix}L\\ k'\end{pmatrix}\right.\right.$$

$$\left.\left.-\xi_\alpha\begin{pmatrix}0\\ k\end{pmatrix}\right)\left(\xi_\beta\begin{pmatrix}L\\ k'\end{pmatrix}-\xi_\beta\begin{pmatrix}0\\ k\end{pmatrix}\right)\right\rangle. \qquad (16)$$

The conditions for absence of internal stresses $(\partial F/\partial e_{\alpha_{L^3}}=\partial F/\partial w_\alpha(k)=0)$ determine the temperature dependence of the structure constants of the lattice. Using the expression (10), we obtain

$$\mathbf{e}=-\mathbf{S}(\mathbf{T}-\mathbf{ba}^{-1}\mathbf{P})v_0^{-1}, \qquad (17)$$

$$\mathbf{w}=-\mathbf{a}^{-1}\mathbf{be}-\mathbf{a}^{-1}\mathbf{P}v_0^{-1}, \qquad (18)$$

where $\mathbf{S}=(\hat{\mathbf{C}}-\mathbf{ba}^{-1}\mathbf{b})^{-1}$ is the elastic-compliance tensor of the crystal.

Just as a change of temperature, isotopic substitution of atoms in the kth sublattice induces a fully symmetric deformation and changes of basis that are given by (17) and (18), in which the tensor $\mathbf{T}$ and vectors $\mathbf{P}$ must be replaced by expressions analogous to (15) and (16) but containing differences of correlation functions corresponding to crystals with different isotopic compositions.

Crystals of the double fluorides LiRF$_4$ have space symmetry group C_{4h}^6, the Bravais lattice is body-centered tetragonal, and the unit cell has a volume $v_0=a^2c/2$ and contains 12 ions, with the coordinates given in Table I. A fully symmetric deformation of the lattice is described by the strain-tensor components $e_1(A_g)=e_{zz}$, $e_2(A_g)=(e_{xx}+e_{yy})/2$ and linear combinations of the displacements $w_\alpha(F_i)$ of the fluoride sublattices, transforming according to the irreducible representation A_g of the factor group C_{4h} of the lattice. As the basis in the space of fully symmetric displacements we have chosen the increments of the dimensionless structure constants that determine the coordinates of the fluorine ions in the cell (see Table I): $w_1=\delta x$, $w_2=\delta y$, $w_3=\delta z$. The change of the specific free energy of the crystal under a fully symmetric deformation takes the form

$$F=\frac{1}{2}v_0\sum_{ik}(\hat{C}_{ik}(A_g)e_i(A_g)e_k(A_g)+16b_{ik}e_i(A_g)w_k$$

$$+8a_{ik}w_iw_k)+\sum_i(T_ie_i(A_g)+P_iw_i), \qquad (19)$$

where $T_1=T_{zz}$, $T_2=T_{xx}+T_{yy}$, $P_1=aP_x(F_6)$, $P_2=aP_y(F_6)$, $P_3=cP_z(F_6)$, and $a_{ik}=\varepsilon_i\varepsilon_k m_F D_{ik}V_0^1$ (m_F is the mass of the fluorine atom, $\varepsilon_1=\varepsilon_2=a$, $\varepsilon_3=c$, and D_{ik} is that block of the dynamical matrix that determines the frequencies of the A_g vibrations at the center of the Brillouin zone); the matrix b_{ik} with elements

$$ab_{11}=b_{zzx}(F_6),\quad ab_{21}=b_{xxx}(F_6)+b_{yyx}(F_6),$$

$$ab_{12}=b_{zzy}(F_6),\quad ab_{22}=b_{xxy}(F_6)+b_{yyy}(F_6),$$

$$cb_{13}=b_{zzz}(F_6),\quad cb_{23}=b_{xxz}(F_6)+b_{yyz}(F_6)$$

characterizes the linear relationship between the macrodeformations and microdeformations.

Using (19), in accordance with (17) and (18) we obtain

$$e_i(A_g)=-\sum_j S_{ij}(A_g)\left[T_j-8\sum_{kl}b_{jk}a_{kl}^{-1}P_e\right]v_0^{-1}, \qquad (20)$$

$$w_i=-\sum_{kj}a_{ik}^{-1}b_{jk}e_j(A_g)-\sum_k a_{ik}^{-1}P_kv_0^{-1}, \qquad (21)$$

where $S_{11}(A_g)=S_{33}$, $S_{12}(A_g)=S_{13}$, and $S_{22}(A_g)=\frac{1}{2}(S_{11}+S_{12})$ (S_{ij} are the elastic compliances in the Voigt notation; for LiRF$_4$ crystals they are given in Refs. 17 and 18).

Thus, to calculate the changes $\delta c=ce_1(A_g)$ and $\delta a=ae_2(A_g)$ of the lattice constants and the displacements w_i of the fluorine ions in the cell that result from isotopic substitution of the lithium sublattices, we need the values of the second- and third-order force constants and the correlation functions of the displacements of the ions in crystals of different isotopic compositions. The calculation was performed in the framework of the rigid-ions model developed previously with the aim of describing the forced magnetostriction[19] and Raman-scattering spectra of lithium–rare-earth double fluorides.[13,20,21] The potential energy of the lattice was represented by a sum of pair Coulomb and non-Coulomb interactions between ions with effective charges ek_c (Li$^+$), $3ek_c$ (Ho^{3+}), and $-ek_c$ (F^-) [$k_c^2=0.8$, and e is the proton charge]. Non-Coulomb inter-

TABLE II. Parameters of the non-Coulomb interactions in the $LiHoF_4$ crystal.

Type of bond	Bond length, Å	A_{ij}, 10^{-16} J	ρ_{ij}, Å
Li^+–F^-	1,895	0,7734	0,25030
Ho^{3+}–F^-	2,242	2,4774	0,30614
Ho^{3+}–F^-	2,289	2,2240	0,31251
F^-–F^-	less than 2.7	4,346	0,2483
F^-–F^-	greater than 2.7	4,605	0,2483

actions were introduced between Li^+–F^- nearest neighbors (four bonds per lithium ion), F^-–F^- at interionic distances shorter than 3 Å, and Ho^{3+}–F^- (for the two nearest coordination shells containing four fluorine ions each), in the form of Born–Mayer potentials with an exponential dependence on the interionic distance: $\varphi_{ik}(r)=A_{ik}\exp(-r/\rho_{ik})$. The parameters of the non-Coulomb interactions, given in Table II, are recovered from the second-order force constants obtained by comparison of the calculated and measured frequencies of the vibrations of $LiRF_4$ crystals with zero wave vector.[19,20] Other properties of $LiRF_4$ crystals are also described satisfactorily in the framework of this model;[21] amongst the deficiencies of the model is the fact that the requirements that the quantities $b_{\alpha\beta,\gamma}(k)$ [see (12)] be symmetric under interchange of the indices α and β and that the quantities $[\alpha\beta, \gamma\delta]$ [see (14)] be symmetric under interchange of the index pairs $\alpha\beta$ and $\gamma\delta$ (from the condition of invariance of the potential energy under rotations of the lattice) are fulfilled only approximately—the error is up to 20%.

The frequencies and polarization vectors of vibrations of $^6LiHoF_4$ and $^7LiHoF_4$ crystals were calculated for 800 wave vectors distributed uniformly over the Brillouin zone (159 points in its irreducible part, constituting 1/8 of the volume of the zone). In Table III we present the calculated frequencies of vibrations at the center of the zone, in which the lithium sublattices participate, and the corresponding experimental data for samples with the natural content of the lithium isotopes.[21] In samples enriched with the isotope ^6Li we may expect shifts of up to 20 cm^{-1} in certain lines in the Raman light-scattering and infrared-absorption spectra, as can be seen from Table III.[1] The imaginary parts of the Green functions of the regular lattices were calculated at n ($n=500$) points on the frequency axis, at the values $\omega_p^2=(\omega_0^2/n)(p-1/2)$ ($p=1,2,\ldots,n$), where $\omega_0(E_uLO)$ is the limiting frequency of the lattice vibrations (580 cm^{-1} in the $^7LiHoF_4$ crystal), using the relation

$$\mathrm{Im}\sum_{\mathbf{q}j}\frac{\varphi(\mathbf{q}j)}{\omega_p^2-\omega_j^2(q)}=\frac{\pi n}{\omega_0^2}\sum_{\mathbf{q}j}\mathrm{Re}\,\varphi(\mathbf{q}j)\left[\mathbf{e}\left(\omega_j^2(\mathbf{q})-\omega_p^2+\frac{\omega_0^2}{2n}\right)-\theta\left(\omega_j^2(\mathbf{q})-\omega_p^2-\frac{\omega_0^2}{2n}\right)\right], \tag{22}$$

Here $\theta(x)$ is the step function and $\varphi(\mathbf{q}, j)=\varphi(-\mathbf{q}, j)^*$. Analogous calculations were also performed using a linear scale of frequencies. In Fig. 1, as an example, we give the results of a calculation of the spectral densities $\mathrm{Im}\,G_{xx}(^7\mathrm{Li},^7\mathrm{Li})$ and $-\mathrm{Im}\,G_{xx}(^6\mathrm{Li},^6\mathrm{Li})$ of the displacements of the lithium ions. It can be clearly seen that decrease of the mass of the lithium ions is manifested principally in the region of frequencies of the optical vibrations, and in the $^6LiHoF_4$ crystal the spectrum of the optical modes is shifted toward higher frequencies by 20–30 cm^{-1}.

In calculating anharmonic isotope effects (in particular, the internal stresses T_i and the forces P_i acting on the fluorine sublattices), we took into account only terms containing the differences of the autocorrelation functions of the displacements of the ions and the correlation functions of nearest Li^+–F^- and Ho^{3+}–F^- neighbors: $\Delta_{\alpha\beta}(kk')=\langle\xi_\alpha|k|\xi_\beta(k')\rangle{}^6\mathrm{LiHoF}_4-\langle\xi_\alpha(k)\xi_\beta(k')\rangle{}^7\mathrm{LiHoF}_4$. The results of the calculations of $\Delta_{\alpha\beta}(kk')$ and the correlation functions of the $^7LiHoF_4$ lattice at temperatures 0 K, 100 K, and 300 K [see (9)] are presented in Table IV. The values obtained for the mean-square displacements at

TABLE III. Calculated and measured[13–15] vibrational frequencies $\omega(\Gamma_i)$ (in cm^{-1}) at the center of the Brillouin zone of $LiRF_4$ crystals.

Γ	i	Calculation		Experiment		Γ	i	Calculation		Experiment	
		$^6LiHoF_4$	$^7LiHoF_4$	$LiHoF_4$	$LiYF_4$			$^6LiHoF_4$	$^7LiHoF_4$	$LiHoF_4$	$LiYF_4$
B_g	1	155	150	157	177	A_u	1	0	0	0	0
	2	230	229	216	248	(TO)	2	220	218	206	192
	3	329	319	328	329		3	241	241	238	252
	4	401	401	377	382		4	312	286	352	396
	5	485	464	432	427		5	443	440	382	489
E_g	1	120	120	129	153	E_u	1	0	0	0	0
	2	177	177	180	199	(TO)	2	128	128	142	144
	3	341	341	332	329		3	266	266	282	262
	4	402	391	368	368		4	339	335	323	314
	5	461	444	457	446		5	427	403	415	413

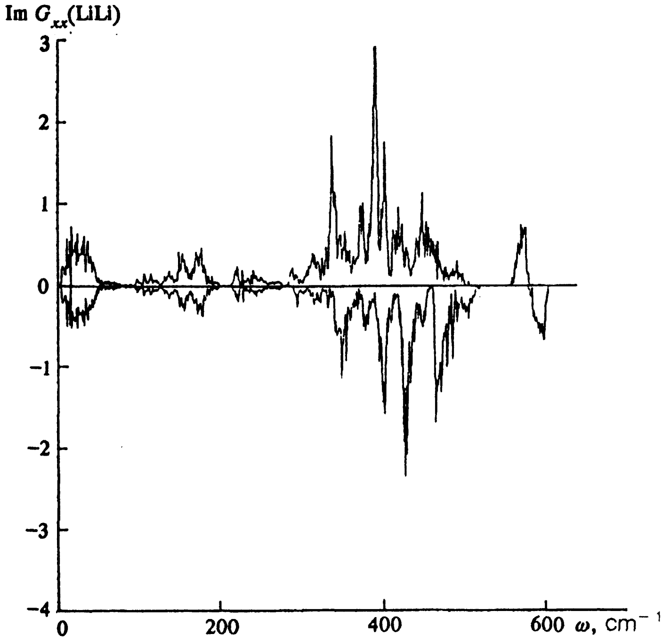

FIG. 1. Spectral densities of the displacements of lithium ions in the basal plane of crystals of ^{7}LiHoF$_4$ (upper) and ^{6}LiHoF$_4$ (lower).

$T=100$ K and $T=300$ K agree qualitatively with the results, given in Ref. 22, of an analysis of neutron scattering in an LiTbF$_4$ crystal. The model introduced for the lattice dynamics and the approximations used were also tested by a calculation of the thermal expansion of LiHoF$_4$ crystals. Confining ourselves to allowance for the anharmonic force constants corresponding to the interactions of only the most closely spaced F$^-$–Li$^+$ and F$^-$–Ho^{3+} ion pairs, we can write the thermal forces acting on the fluorine sublattices in the form

$$\begin{aligned} P_\gamma(\mathrm{F}_6)=-\tfrac{1}{2}[&\Phi'''_{\alpha\beta\gamma}(\mathrm{F}_6\mathrm{F}_6\mathrm{Li}_1)f_{\alpha\beta}(\mathrm{F}_6\mathrm{Li}_1)\\ &+\Phi'''_{\alpha\beta\gamma}(\mathrm{F}_6\mathrm{F}_6\mathrm{Ho}_1)f_{\alpha\beta}(\mathrm{F}_6\mathrm{Ho}_1)\\ &+\Phi'''_{\alpha\beta\gamma}(\mathrm{F}_6\mathrm{F}_6\mathrm{Ho}_2)f_{\alpha\beta}(\mathrm{F}_6\mathrm{Ho}_2)], \end{aligned} \tag{23}$$

where

$$f_{\alpha\beta}(\mathrm{F}_6k)=\langle(\xi_\alpha(\mathrm{F}_6)-\xi_\alpha(k))(\xi_\beta(\mathrm{F}_6)-\xi_\beta(k))\rangle. \tag{24}$$

In the framework of this approximation, we obtain for the internal thermal stresses the expression

$$\begin{aligned} T_{\alpha\beta}=4[&\Phi'''_{\gamma\delta\alpha}(\mathrm{F}_6\mathrm{F}_6\mathrm{Li}_1)X_\beta(\mathrm{Li}_1\mathrm{F}_6)f_{\gamma\delta}(\mathrm{F}_6\mathrm{Li}_1)\\ &+\Phi'''_{\gamma\delta\alpha}(\mathrm{F}_6\mathrm{F}_6\mathrm{Ho}_1)X_\beta(\mathrm{Ho}_1\mathrm{F}_6)f_{\gamma\delta}(\mathrm{F}_6\mathrm{Ho}_1)\\ &+\Phi'''_{\gamma\delta\alpha}(\mathrm{F}_6\mathrm{F}_6\mathrm{Ho}_2)X_\beta(\mathrm{Ho}_2\mathrm{F}_6)f_{\gamma\delta}(\mathrm{F}_6\mathrm{Ho}_2)]. \end{aligned} \tag{25}$$

The matrix components a_{ik} and b_{ik} needed for the calculation of the thermal displacements of the sublattices and the thermal deformations by means of Eqs. (20) and (21) are given in Table V. The changes of the internal forces and stresses following a one-degree change of the temperature of the LiHoF$_4$ crystal (in the temperature range 250–300 K), calculated in accordance with (23) and (25), are pre-

TABLE IV. Correlation functions of displacements of ions in LiHoF$_4$ crystals.

$kk'\alpha\beta$			$\langle\xi_\alpha(k)\xi_\beta(k')\rangle$, 10^{-2} Å^2			$\Delta_{\alpha\beta}(kk')$	$\delta^{6-7}_{\alpha\beta}(kk')$	$\delta^{7-6}_{\alpha\beta}(kk')$
			T = 300 K	100 K	0 K	$T=0$ K, units of 10^{-6} Å^2		
1	1	xx	2,64	1,22	0,73	475,3	482,2	−489,0
1	1	zz	2,47	1,20	0,86	573,8	577,1	−584,1
1	2	xx	1,78	0,60	0,11	6,2	11,0	−11,8
1	2	yy	1,80	0,61	0,11	9,5	14,9	−12,0
1	2	zz	0,96	0,33	0,09	12,9	24,0	−15,8
1	2	$(xy)^*$	−0,09	−0,03	−0,02	−3,4	−3,8	3,5
1	2	(xz)	−0,30	−0,10	−0,02	0,7	−0,5	0,4
1	2	(yz)	−0,08	−0,03	0,01	2,1	3,0	−3,0
2	2	xx	2,63	1,02	0,44	−0,1	1,3	−0,9
2	2	yy	2,70	1,04	0,43	1,0	1,6	−0,9
2	2	zz	1,64	0,69	0,39	−0,4	1,7	−0,9
2	2	(xy)	−0,79	−0,28	−0,15	−3,9	−0,5	0,7
2	2	(xz)	−0,69	−0,24	−0,14	−2,8	0,0	0,4
2	2	(yz)	0,73	0,26	0,16	3,4	0,5	−0,3
3	3	xx	2,10	0,72	0,15	−2,6	—	—
3	3	zz	1,10	0,39	0,11	−3,0	—	—
2	3	xx	1,72	0,58	0,08	−3,3	—	—
2	3	yy	1,77	0,59	0,08	−2,7	-	—
2	3	zz	0,87	0,29	0,05	−3,7	—	—
2	4	xx	1,77	0,59	0,08	−3,3	—	—
2	4	yy	1,73	0,58	0,08	−3,4	—	—
2	4	zz	0,89	0,30	0,06	−3,0	—	—

Notes: $^*(\alpha\beta)=\alpha\beta+\beta\alpha$; the coordinates of the ions are Li(0,0,0) ($k=1$), F_6 (x,y,z) ($k=2$), Ho(1/2, 1/2, 0) ($k=3$), and Ho(1/2, 0, 1/4) ($k=4$).

TABLE V. Constants of the relationship between the microdeformations and macrodeformations, and parameters of the elastic energy of the sublattices (in units of 2×10^{-17} J).

i	k	v_0b_{ik}	$v_0a_{ik} = v_0a_{ki}$
1	1	-0,1617	2,3408
1	2	-0,0124	0,625
1	3	-0,2064	1,600
2	1	-0,5103	—
2	2	-0,2392	0,883
2	3	-0,0639	-0,530
3	3	—	4,361

sented in Table VI. The values finally obtained for the thermal-expansion coefficients ($\alpha_1=de_1(A_g)/dT$ along the symmetry axis, and $\alpha_2=de_2(A_g)/dT$ in the basal plane of the lattice) are in satisfactory agreement with the measurement data available in the literature (see Table VI). The substantial discrepancy between the theoretical estimates and the measurements of the rates of change dw_i/dT of the coordinates of the fluorine ions in the unit cell of the $LiTbF_4$ crystal from 100 K to 300 K (Ref. 22) is due to the neglect of the interactions between the fluoride ions, but this circumstance does not affect the estimates of the thermal-expansion coefficients, since the corresponding internal-deformation contributions to the α_i do not exceed 5% of the values of the α_i.

As can be seen from Table IV, upon substitution of ^{7}Li by the isotope ^{6}Li in the $LiHoF_4$ lattice it is principally the autocorrelation functions of the displacements of the lithium ions that change, and at $T=0$ K their relative change amounts to $\sim6.6\%$. The corresponding terms in the internal forces and stresses induced by the change of mass of the lithium sublattices are equal to

$$\Delta P_\gamma(\mathrm{F}_6)\sim-\frac{1}{2}\sum_{Lk\alpha}\Phi'''_{\alpha\alpha\gamma}(\mathrm{F}_6\mathrm{F}_6\mathrm{Li}_k(L))\Delta_{\alpha\alpha}(11),$$

$$\Delta T_{\alpha\alpha}\sim\sum_{Lk\beta}\Phi'''_{\beta\beta\alpha}\left(\mathrm{Li}_1\mathrm{Li}_1{L\atop k}\right)X_\alpha\left({L\atop k},\mathrm{Li}_1\right)\Delta_{\beta\beta}(11).$$

The summation, over the lattice, of the contributions of the Coulomb interaction to the force constants $\Sigma_L\Phi^{C'''}_{\alpha\beta\gamma}\left({0\;0\;L\atop k\;k\;k'}\right)$ was carried out directly, and the lattice sums $\Sigma_L\Phi^{C'''}_{\alpha\beta\gamma}\left({c\;0\;L\atop k\;k\;k'}\right)X_\delta\left({L\;0\atop k'\;k}\right) = (\alpha\beta\gamma,\delta|kk')$ were calculated by the Ewald method (to check the results we used the identity

$$\sum_{\alpha\beta}\sum_{L}(\alpha\alpha\beta\beta|kk')=24\frac{\pi}{v_0}e(k)e(k'),\qquad(26)$$

where $e(k)$ are the ion charges). The isotopic internal forces and stresses obtained with allowance for all the changes $\Delta_{\alpha\beta}(kk')$ [given in Table IV] of the correlation functions, and also the consequent displacements $\Delta\mathbf{w}=-\mathbf{a}^{-1}\Delta\mathbf{P}$ of the sublattices and the fully symmetric deformations e_i in the $^6LiHoF_4$ crystal relative to the $^7LiHoF_4$ lattice at $T=0$ K, are presented in Table VI. We note that, in contrast to the case of thermal expansion, in the case of isotopic substitution the internal deformations Δw substantially renormalize the effective stresses in the lattice (the values of $-\mathbf{b}\mathbf{a}^{-1}\Delta\mathbf{P}$ [see (17)] are given in Table VI). The isotopic deformation is substantially anisotropic, and the calculated differences of the lattice constants of the $^6LiHoF_4$ and $^7LiHoF_4$ lattices are equal to $\Delta a=ae_2(A_g)=7.2$ and $\Delta c=ce_1(A_g)=-0.6$, in units of 10^{-4} Å.

2. LOCAL STRUCTURE OF A LATTICE WITH AN ISOLATED IMPURITY ISOTOPE IN THE LITHIUM SUBLATTICE

The method of calculating the static displacements $\delta\mathbf{u}$ in a locally deformed lattice that arise from the introduction of one ion-isotope is based, as in the preceding section, on seeking the minimum of the free energy of the crystal with allowance for anharmonic terms in the average potential energy (1) of the lattice.

We denote by ξ' the dynamic displacements of the atoms in a lattice with an isolated mass defect at the site $L==$, $k=0$ (Li_1). From the condition for equilibrium of the lattice we obtain

TABLE VI. Thermal and isotopic changes of the structure of the $LiHoF_4$ lattice.

Internal forces and displacements of the sublattices					
i	$\frac{dP_i}{dT}$, 10^{-23} J K^{-1}	$\frac{dw_i}{dT}$, 10^{-6} K^{-1}		ΔP_i, 10^{-21} J	Δw_i, 10^{-6}
		calculation	experiment		
1	-0,631	3,8	0,5*	-1,666	-17,6
2	1,106	2,1	6,1*	-0,977	92,8
3	-8,760	0,6	-1,4*	-2,082	41,6
Internal stresses and uniform deformations					
i	$\frac{dT_i}{dT}$, 10^{-21} J K^{-1}	α_i, 10^{-6} K^{-1}		ΔT_i, 10^{-21} J	e_i, 10^{-4}
		calculation	experiment		
1	-0,518	9,1	8,3** 14***	-1,578 (-1,101)	-0,056
2	-1,215	18,4	18,3** 21***	-5,149 (-2,537)	1,377

Note: The contributions to the isotopic stresses from the internal deformation are given in parentheses. The experimental data on the thermal expansion refer to the crystals $LiTbF_4$ (*—Ref. 22), $LiY_{0.5}Tb_{0.5}F_4$ (**—Ref. 17), and $LiYF_4$ (***—Ref. 23).

$$\delta\mathbf{u}=\tfrac{1}{2}\mathbf{G}(\omega=0)\Phi'''(\langle\xi'\xi'\rangle-\langle\xi\xi\rangle). \tag{27}$$

We introduce the Green function of the defect lattice:

$$\begin{aligned}\mathbf{G}'&=[(\mathbf{m}+\delta\mathbf{m})\omega^2-\Phi'']^{-1}\\ &=\mathbf{G}-\mathbf{G}(1+\delta\mathbf{m}\omega^2\mathbf{G})^{-1}\delta\mathbf{m}\omega^2\mathbf{G},\end{aligned} \tag{28}$$

where $\delta m_{\alpha\beta}\left(\begin{smallmatrix}L & L'\\ k & k'\end{smallmatrix}\right)=\delta m\delta_{\alpha\beta}\delta_{kk'}\delta_{LL'}\delta_{k0}\delta_{L0}$. As our calculations have shown, in ^{7}LiHoF$_4$ and ^{6}LiHoF$_4$ crystals containing isolated ^{6}Li and ^{7}Li atoms, respectively, the conditions for the existence of local vibrations:

$$1+\delta m\omega^2 G_{\alpha\alpha}\left(\begin{matrix}0 & 0\\ 0 & 0\end{matrix}\middle|\,\omega\right)=0 \tag{29}$$

are not fulfilled outside the frequency spectrum of the regular lattice. In this case, the difference of the correlation functions of the displacements of the atoms can be represented, at $T=0$ K, in the form [see (9)]

$$\begin{aligned}\delta&=\langle\xi'\xi'\rangle-\langle\xi\xi\rangle\\ &=-\frac{\hbar}{2\pi}\int \operatorname{Im} G(1+\delta m\omega^2 G)^{-1}\delta m G\omega d\omega^2.\end{aligned} \tag{30}$$

In the approximation of pair interactions we obtain from (27)

$$\begin{aligned}\delta u_\alpha\begin{pmatrix}L\\ k\end{pmatrix}&=-\frac{1}{2}\sum_{L'k'}\sum_{L''k''}G_{\alpha\beta}\left(\begin{matrix}L & L'\\ k & k'\end{matrix}\middle|\,0\right)\\ &\quad\times\Phi'''_{\beta\gamma\delta}\begin{pmatrix}L' & L' & L''\\ k' & k' & k''\end{pmatrix}\left[\delta_{\delta\gamma}\begin{pmatrix}L' & L'\\ k' & k'\end{pmatrix}\right.\\ &\quad+\delta_{\delta\gamma}\begin{pmatrix}L'' & L''\\ k'' & k''\end{pmatrix}-\delta_{\delta\gamma}\begin{pmatrix}L' & L''\\ k' & k''\end{pmatrix}\\ &\quad\left.-\delta_{\delta\gamma}\begin{pmatrix}L'' & L'\\ k'' & k'\end{pmatrix}\right].\end{aligned} \tag{31}$$

The difference of the spectral densities and the corresponding correlation functions of the displacements of the atoms in the defect lattice and regular lattice is a maximum for the defect site, and decreases rapidly with increase of the distance between the atom and the impurity center. In the framework of the lattice-dynamics model considered above we have calculated the displacements of the fluorine ions in the first coordination shell of the impurity lithium isotopes in ^{7}LiHoF$_4$ and ^{6}LiHoF$_4$ crystals, confining ourselves, in the double lattice sum in (31), to the differences $\delta^{m'-m}_{\alpha\beta}(kk')$ (presented in Table IV) of the correlation functions of the displacements of the impurity ion-isotope $^{m'}$Li and its nearest neighbors (four fluorine ions); we have also confined ourselves to allowance for terms containing zero-frequency Green functions, corresponding to the bonds of these four fluorine ions with each other and with their nearest neighbors.

The real parts of the Green functions of the regular lattice were calculated using Cauchy transforms; the calculational errors that arise from taking into account only a comparatively small number of points in the first Brillouin zone were corrected by requiring that the normalization conditions

$$\begin{aligned}\int \operatorname{Im}\Bigg[&(m_k+\delta m_k)G'_{\alpha\alpha}\left(\begin{matrix}0 & 0\\ k & k\end{matrix}\middle|\,\omega\right)\\ &-m_k G_{\alpha\alpha}\left(\begin{matrix}0 & 0\\ k & k\end{matrix}\middle|\,\omega\right)\Bigg]d\omega^2=0\end{aligned} \tag{32}$$

be fulfilled, and that the Green functions at zero frequency in the regular lattice and impurity lattice be equal:

$$\int \operatorname{Im}(\mathbf{G}'-\mathbf{G})\,\frac{d\omega^2}{\omega^2}=0. \tag{33}$$

The spectral density of the displacements of the light isotope ^{6}Li in the ^{7}LiHoF$_4$ lattice increases in the region of high frequencies (the differences of the spectral densities of the displacements of the impurity isotope and principal isotope of lithium in the basal plane of the ^{7}LiHoF$_4$ and ^{6}LiHoF$_4$ crystals are given, as an example, in Figs. 2a and 2b, respectively); the increase of the amplitude of the vibrations as a consequence of the dominant role of the forces of repulsion in the formation of the anharmonic forces leads to an increase of the distance from the light impurity ion to its nearest neighbors. Our calculated results for the displacements of the ion F$_6$ (see Table I) near an isolated ^{6}Li$^+$ impurity ion at the site (0,0,0) are (in units of 10^{-4} Å): $\delta x=3.078$ (-3.050), $\delta y=3.456$ (-3.466), and $\delta z=2.672$ (-2.697), where the figures in parentheses give the corresponding displacements of ions in the first coordination shell of the ^{7}Li$^+$ ion in ^{6}LiHoF$_4$. Thus, the local deformations of the lattice near impurity isotopes ^{6}Li and ^{7}Li in ^{7}LiHoF$_4$ and ^{6}LiHoF$_4$ crystals, respectively, differ essentially only in sign.

3. CRYSTAL FIELD IN ^{6}Li$_x$^{7}Li$_{1-x}$YF$_4$:Ho^{3+} CRYSTALS

In the regular ^{7}LiYF$_4$ lattice the interaction of Ho^{3+} ions (replacing yttrium ions at sites with point symmetry S_4) with the intracrystal field is described by the Hamiltonian (in the crystallographic system of coordinates)

$$H_0=\sum_{p=2,4,6}a_p B_p^0 O_p^0+\sum_{p=4,6}a_p(B_p^4 O_p^4+B_p^{-4}\Omega_p^4), \tag{34}$$

where $O_p^{|k|}$ and $\Omega_p^{|k|}=O_p^{-|k|}$ are Stevens operators, defined in the space of the states $|JJ_z\rangle$ of a multiplet with total angular momentum J (Ref. 24), and $a_2=\alpha_J$, $a_4=\beta_J$, and $a_6=\gamma_J$ are reduced matrix elements, the values of which for the Ho^{3+} ion were calculated in Ref. 25. The crystal-field parameters B_p^k are functions of the interionic distances in the lattice and, upon deformation of the latter, because of the isotopic substitution of the lithium ions, the Hamiltonian of the rare-earth ions in the ^{6}Li$_x$^{7}Li$_{1-x}$YF$_4$ crystal takes the form

$$H_{\mathrm{cr}}=H_0+\delta H+\Delta H(\Gamma_1)+\Delta H(\Gamma_2)+\Delta H(\Gamma_{34}). \tag{35}$$

Here δH is a term that is the same for all sites of the yttrium sublattices, and is due to the change of the structure constants of the crystal; it has the same structure as

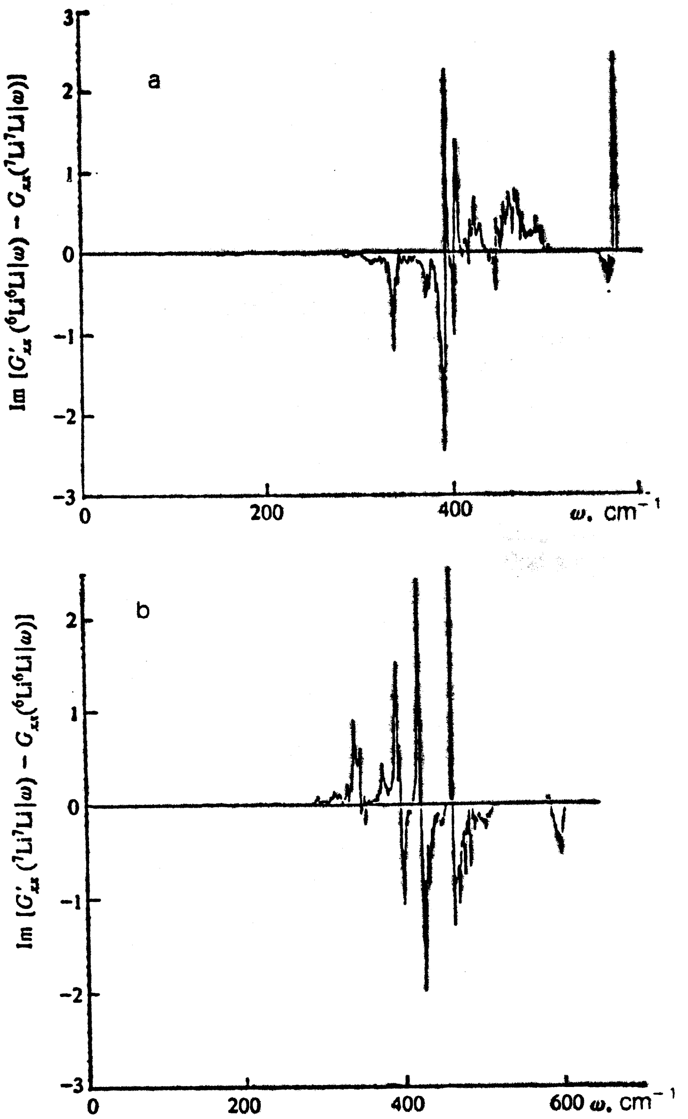

FIG. 2. a—Difference of the spectral densities of the displacements of lithium isotopes in ^{7}LiHoF$_4$ crystals; b—difference of the spectral densities of the displacements of lithium isotopes in ^{6}LiHoF$_4$ crystals.

the operator (34); the parameters δB_p^k of the operator $\delta H=\Sigma_{pk}\delta B_p^k a_p O_p^k$ can be expressed in terms of the constants of the electron–deformation interaction that determine the change of the energy of the rare-earth ion under fully symmetry macrodeformations and microdeformations:

$$\delta H=\sum_{pk} a_p O_p^k\left[\sum_{i=1,2} e_i(A_g)B_{pi}^k(A_g)+\sum_{i=1}^{3}\Delta w_i B_{pi}^{k'}(A_g)\right]. \tag{36}$$

The values of the components $e_i(A_g)$ of the uniform-strain tensor and of the displacements Δw_i of the fluorine sublattices depend on the relative concentrations of the lithium isotopes. The operators $\Delta H(\Gamma_i)$ determine the interaction of the rare-earth ions with the components of the nonuniform static crystal field that correspond to local deformations of symmetry Γ_i (classified according to irreducible representations of the point group S_4) that arise from the random distribution both of the lithium isotopes and of the rare-earth impurity ions over the lattice sites. In the case of a small concentration of one of the lithium isotopes, e.g., ^{6}Li, the main contribution to ΔH is made by displacements of the eight fluorine ions in the immediate neighborhood of the rare-earth ion. Each of these eight fluorine ions appears in the first coordination shell of one of the eight lithium sites with coordinates (relative to the rare-earth ion)

$$\mathrm{Li}_1(\pm 1/2,1/2,0),\quad (\pm 1/2,-1/2,0),$$

$$\mathrm{Li}_2(\pm 1/2,0,1/4),\quad (0,\pm 1/2,-1/4).$$

The distribution of the ^{6}Li isotopes over these sites determines the structure of the operator $\Delta H(\Gamma_i)$. Isotopic effects in the energy spectrum can be considered in the framework of perturbation theory. We can disregard perturbations of symmetry Γ_{34}, since in the first approximation they are not effective. Perturbations of symmetry Γ_1 (which have the same structure as the operator H_0) and Γ_2 will be determined by the parameters $\Delta B_p^k(R_i|\Gamma_j)$ in the operators

$$\Delta H_i(\Gamma_j)=\sum_{pk} a_p \Delta B_p^k(R_i|\Gamma_j)O_p^k \tag{37}$$

corresponding to rare-earth ions at the sites R_1 (1/2,1/2,0) and R_2 (1/2,0,1/4) near an isolated ^{6}Li isotope at the site (0,0,0) in the ^{7}LiYF$_4$ lattice. The parameters $\Delta B_p^k(R_i|\Gamma_j)$ are linear functions of the components δx, δy, and δz of the displacement vector of the ion F$_6$ and were considered in Sec. 2 of this paper. Assuming that the deformations induced by individual impurity isotopes are additive, and taking into account that under rotations through $\pi/2$ about the symmetry axis of the lattice the operators $\Delta H_i(\Gamma_1)$ are invariant while the operators $\Delta H_i(\Gamma_2)$ change sign, we obtain

$$\Delta H(\Gamma_1)=n_1\Delta H_1(\Gamma_1)+n_2\Delta H_2(\Gamma_1), \tag{38}$$

$$\Delta H(\Gamma_2)=m_1\Delta H_1(\Gamma_2)+m_2\Delta H_2(\Gamma_2), \tag{39}$$

where the n_i are the numbers of sites of the type Li$_i$ that are occupied by ^{6}Li isotopes ($0\leqslant n_i\leqslant 4$), and $m_i=0$, ± 1, ± 2. The relative number of holmium ions with a definite energy spectrum—in particular, with the Hamiltonian (38)—can be represented by a product of binomial distributions:

$$P_{n_1n_2}\sim C_4^{n_1}C_4^{n_2}x^{n_1+n_2}(1-x)^{8-n_1-n_2}. \tag{40}$$

The numerical values given in Tables VII and VIII for the parameters $\Delta B_p^k(R_i|\Gamma_j)$ of the operator (37) and $\delta B_p^k=\delta B_{pe}^k+\delta B_{pw}^k$, where δB_{pe}^k and δB_{pw}^k are respectively the contributions of the uniform deformation and displacements of the sublattices [see (36)], were obtained in the framework of the model of exchange charges.[12] It was demonstrated previously that the Stark structure of the spectra of the rare-earth ions in crystals of lithium–rare-earth double fluorides can be described satisfactorily by a one-parameter variant of the model with allowance for the interaction of the $4f$-electrons with the fields of point charges, point dipoles, and parametrized exchange charges

TABLE VII. Crystal-field parameters and their changes upon isotopic substitution of lithium ions in the ^{7}LiHoF$_4$ crystal (in cm^{-1}).

p	k	B_p^k		δB_{pe}^k	δB_{pw}^k	δB_p^k	$\Delta B_p^k(i)$	
		experiment[26]	calculation				$i=1$	$i=2$
2	0	189,3	177	–0,195	0,107	–0,088	0,0629	0,0359
4	0	–78,3	–85	0,072	–0,262	–0,190	–0,0323	–0,0183
6	0	–3,3	–2,8	–0,006	0,043	0,037	0,0119	–0,0044
4	4	–657	–699	0,318	–0,775	–0,457	–0,0929	–0,0564
4	–4	–568	–604	0,095	0,293	0,388	–0,1478	0,0268
6	4	–322	–333	0,202	–0,793	–0,591	–0,0808	–0,0941
6	–4	–253	–279	0,230	–0,264	–0,034	–0,1036	0,0402

proportional to the squares of the overlap integrals of the wave functions of the $4f$-electron with the wave functions of the ligands.[19] As can be seen from Table VII, the calculated parameters B_p^k (in the model of exchange charges) of the static crystal field agree well with the results of an analysis of the measured optical spectrum of the LiHoF$_4$ crystal,[26] and also differ little from the parameters of the crystal field in activated LiYF$_4$:Ho^{3+} crystals.[27] The coupling constants of the rare-earth ions with the fully symmetric deformations and the internal deformations, used in the calculation of the parameters δB_p^k, were tested earlier in an analysis of the results of piezospectroscopic investigations[28] and by investigations of coupled electron-phonon excitations[21] in LiRF$_4$ crystals. The data of Tables VII and VIII are used below in a calculation of the isotopic structure of the optical spectrum of holmium ions in the LiYF$_4$ lattice.

4. ISOTOPE SHIFTS OF THE HYPERFINE COMPONENTS IN THE OPTICAL ABSORPTION SPECTRA OF ^{6}Li$_x$^{7}Li$_{1-x}$YF$_4$:Ho CRYSTALS

With the aim of investigating spectral isotopic effects, crystals of LiYF$_4$:Ho (0.1 at.%) were grown with different isotopic compositions in the lithium. The compound Li$_2$CO$_3$, with certificated isotopes of lithium, was used as the starting material, and was converted to LiF by a dry method. Stockbarger's method was used to obtain from a mixture of the fluorides of lithium, holmium, and yttrium a single-isotope crystal of ^{7}LiYF$_4$ (the content of the isotope ^{6}Li did not exceed 0.5 at.%), a crystal of ^{6}Li$_{0.9}$^{7}Li$_{0.1}$YF$_4$ enriched in the isotope ^{6}Li, and crystals with the natural mixture of isotopes (7.42% of the isotope ^{6}Li).[2]

TABLE VIII. Parameters of the rhombic component of the crystal field acting on Ho^{3+} ions at the sites (1/2,1/2,0) for $i=1$ and (1/2,0,1/4) for $i=2$ near the isotope ^{6}Li(0,0,0) in the ^{7}LiYF$_4$ crystal.

p	k	$\Delta B_p^k(1)$, 10^{-4} cm^{-1}	$\Delta B_p^k(2)$, 10^{-4} cm^{-1}
2	2	–2178	–1966
2	–2	1887	–1864
4	2	–709	–887
4	–2	1474	–1752
6	2	558	–314
6	–2	–1129	–364
6	6	722	37
6	–6	78	162

The energy spectrum of Ho^{3+} ions in a crystal field of symmetry S_4 consists of Γ_1 and Γ_2 singlets and Γ_{34} doublets. The ground state in the lower multiplet $^5I_8$ is a Γ_{34} doublet, and the nearest excited state (with energy 7 cm^{-1}) is a Γ_2 singlet.

The absorption spectra were measured at temperatures 2–5 K with a resolution of 0.004 cm^{-1} on a BOMEM DA3.002 Fourier spectrometer. The frequencies of the absorption lines from the ground state $\Gamma_{34}^1(^5I_8)$ to sublevels of the multiplets ^5I_J ($J=7,6,5,4$) are given in Table IX. The inhomogeneous broadening of the spectral lines in the samples investigated by us was extremely small, and this made it possible to observe the hyperfine structure of the transitions.[29] The energy of interaction of the Ho^{3+}-ion nucleus, with spin $I=7/2$, with the electron shell can be represented largely by the Hamiltonian $H_{\rm hfs}=A_J(\mathbf{J}\cdot\mathbf{I})$. The diagonal matrix elements of the operator $\mathbf{J}$ are nonzero only on the doublet wave functions

$$|\Gamma_{34}^{\pm}\rangle=a_1^{\pm}|J,\pm 1\rangle+a_3^{\pm}|J,\mp 3\rangle+a_5^{\pm}|J,\pm 5\rangle+...$$

$(a_M^+=(a_M^-)^*$, and $\langle +|J_z|+\rangle=-\langle -|J_z|-\rangle)$, and in the first approximation the hyperfine sublevels of the doublet form a structure with equally spaced energies $\pm A_J\langle +|J_z|+\rangle m$, where $m=\pm 1/2,...,\pm 7/2$ are the z-components of the nuclear angular momentum. In the "pure" form, eight hyperfine components of the singlet–doublet transition are observed only in the ^{7}LiYF$_4$ crystal with homogeneous isotopic composition (see Fig. 3), and in the samples of mixed composition, containing isotopes ^{7}Li and ^{6}Li, the hyperfine components of the Γ_1–Γ_{34} and Γ_2–Γ_{34} transitions are split into individual narrow lines (with half-width up to 0.007 cm^{-1}). This isotopic structure of the hyperfine components has equal spacing in most cases; its period is given in Table X for a number of allowed structures and amounts to 0.01–0.03 cm^{-1}.

The isotopic shifts of the Stark sublevels are equal in the first approximation to the diagonal matrix elements of the operator $\delta H+\Delta H(\Gamma_1)$ [see (35) and (38)] on the eigenfunctions of the operator H_0. The latter were obtained with the crystal-field parameters B_p^k from Ref. 26, referred to the crystallographic axes in accordance with the results of the calculation of the ratio B_4^4/B_4^{-4} in the model of

TABLE IX. Energies E of the Stark sublevels of multiplets (reckoned from the lowest sublevel, the energy of which is given in brackets; ΔE are the differences of the calculated and measured sublevel energies in the crystal field) and isotopic shifts of the lines of the hyperfine structure in the absorption spectra of Ho^{3+} ions in $^6LiYF_4$ and $^7LiYF_4$ crystals.

i	α	$E(\Gamma_i^\alpha)$, cm^{-1}	ΔE, cm^{-1}	$\delta\nu$, 10^{-3} cm^{-1}	
				experiment	calculation
Multiplet $^5I_7$ (5152.3 cm^{-1})					
2	1	0,0	0,3	81	87
34	1	3,4	2,6	60 92	60 113*
1	1	10,5	5,9	69	63
2	2	11,0	0,0	76	87
34	2	32,4	−0,2	99 130	118 171*
1	2	53,8	−9,2	40	38
34	3	75,5	2,0	– 130	147 200*
2	3	80,3	2,3	200 ± 100	132
2	4	138,7	−4,2	200 ± 100	112
34	4	140,6	−1,3	– 220	127 180*
1	3	140,8	−1,2	± 200	136
Multiplet $^5I_4$ (13187.5 cm^{-1})					
1	1	0,0	4,6	60	76
34	1	81,5	2,9	– 60¹⁾	73 126
2	1	133,0	7,4	50¹⁾	11
1	2	152,6	−1,2	130¹⁾	177
2	2	162,7	−9,3	—	−37
34	2	219	−3,6	—	117
1	3	351,5	−11,1	—	330
Multiplet $^5I_6$ (8670.9 cm^{-1})					
2	1	0,0	7,4	70	90
1	1	2,4	0,2	60	65
34	1	9,4	−0,8	– 96	64 117*
34	2	15,0	−2,0	50 84	75 128*
2	2	16,8	8,4	134	185
1	2	26,5	−8,5	55	55
2	3	31,1	−0,6	138	182
1	3	98,1	8,0	100	114
34	3	112,8	−0,8	±80 130	124 177*
2	4	125,7	−7,6	190	136
Multiplet $^5I_5$ (11241.6 cm^{-1})					
34	1	0,0	2,8	80 125	74 127*
1	1	5,6	−5,7	68	67
34	2	8,4	3,9	70 110	162 215*
2	1	12,4	−8,2	85	83
1	2	14,0	−9,3	50	59
1	3	59,4	22,0	58	112
34	3	88,4	−2,9	– –	116 169*
2	2	94,4	−6,4	± 40	

Notes: The values marked¹⁾ have accuracy ±40; the values marked with an asterisk are the changes of the frequencies of the transitions to the doublets Γ_{34}^1 from the level $\Gamma_2^1(^5I_8)$. The accuracy of the measurements of the isotope shifts was in the range from 0.001 cm^{-1} to 0.01 cm^{-1} (if not indicated otherwise) for the different lines.

exchange charges (see Table VII). The difference between the Stark-sublevel energies obtained with the use of the operator (34) and the measured energies (see the corresponding differences ΔE in Table IX) is due to the neglect of mixing of states of the same symmetry from different multiplets by the crystal field, to the neglect of the effects of electron–electron correlations,[30] and to the neglect of level shifts due to the electron–phonon interaction. The shift of the ith energy level of the rare-earth ion in the crystal on account of the interaction of the $4f$-electrons with the lattice vibrations can be written in the form ($T=0$ K)

$$\Delta\varepsilon_i=-\frac{\hbar}{2\pi}\sum_j\sum_{LL'kk'}\left\langle i\left|V_\alpha\begin{pmatrix}L\\k\end{pmatrix}\right|j\right\rangle \times\left\langle j\left|V_\beta\begin{pmatrix}L'\\k'\end{pmatrix}\right|i\right\rangle \int\frac{\operatorname{Im}G_{\alpha\beta}\left(\begin{matrix}L & L'\\k & k'\end{matrix}\middle|\omega\right)d\omega^2}{\omega(E_j-E_i+\hbar\omega)}, \tag{41}$$

where $V_\alpha(\begin{smallmatrix}L\\k\end{smallmatrix})$ are the electron operators in the Hamiltonian $H_{e-ph}=\sum_{Lk}V_\alpha(\begin{smallmatrix}L\\k\end{smallmatrix})\xi_\alpha(\begin{smallmatrix}L\\k\end{smallmatrix})$ of the electron–phonon interaction. As an example, using the electron–phonon interaction constants obtained in the model of exchange charges, and the results of calculations of the lattice Green functions, we have calculated rigorously the contributions to the shift of the level Γ_2^1 in the multiplet $^5I_7$ that arise from vibrations of one of the fluorine ions of type F_1 ($\Delta\varepsilon=-0.63$ cm^{-1}) or F_6 ($\Delta\varepsilon=-0.58$ cm^{-1}) nearest to the Ho^{3+} ion at the site (0,0,1/2), so that the total displacement at $T=0$ K is of the order of 4 cm^{-1}. For the crystals of mixed isotopic composition the change of this shift on account of the change of the spectral density of the vibrations is equal to $(2\text{–}5)\times10^{-4}$ cm^{-1}, while that on account of the changes of the coupling constants of the $4f$-electrons with phonons is $(7\text{–}20)\times10^{-4}$ cm^{-1}. These values are substantially smaller than the measured isotope shifts. In the Hamiltonian of the electron-vibrational interaction, which is bilinear in the phonon creation and annihilation operators, it

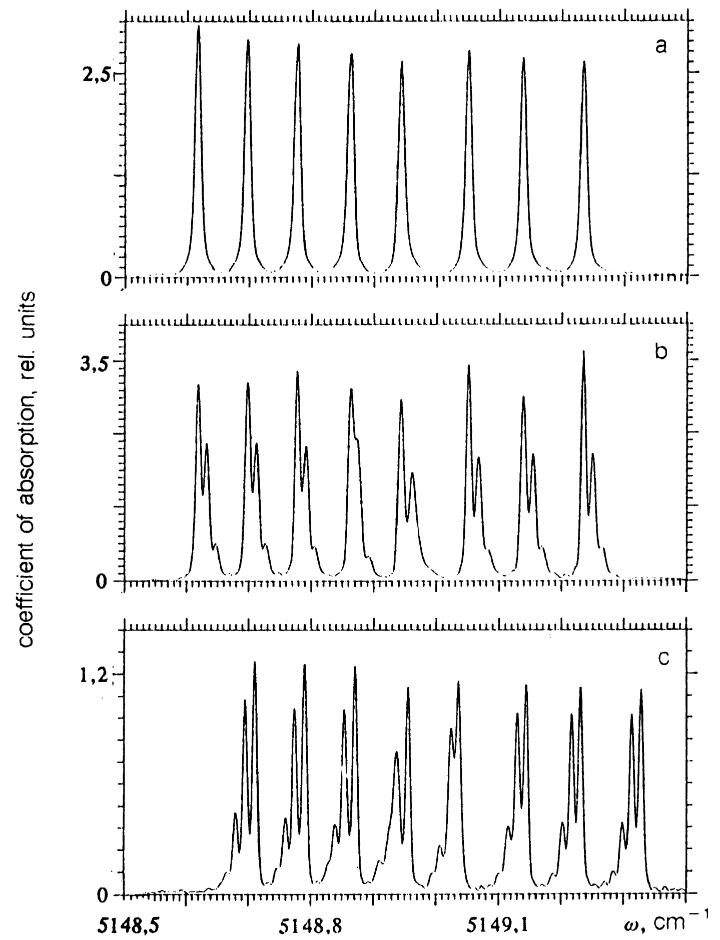

FIG. 3. Hyperfine components of the transition $\Gamma_2^1(^5I_8)$–$\Gamma_{34}^1(^5I_7)$ in (a) ^{7}LiYF$_4$, (b) ^{6}Li$_{0.0742}$^{7}Li$_{0.9258}$YF$_4$, and (c) ^{6}Li$_{0.9}$^{7}Li$_{0.1}$YF$_4$. The polarization is **E**, **H**⊥ *c*.

is sufficient to take into account the terms corresponding to displacements of the impurity lithium isotope. The corresponding contributions made to the displacements of the energy levels of the Ho^{3+} ion by the difference $\delta_{\alpha\alpha}^{6-7}(\mathrm{Li})$ of the mean-square displacements can be estimated easily, since the interaction of the $4f$-electrons with lithium ions represents an interaction with a field of point charges. The magnitudes of these contributions do not exceed 10^{-3} cm^{-1}, and the previously considered[2] mechanism of the isotope shift of the spectral lines is not effective in the case of an inhomogeneous isotopic composition of the matrix.

The rhombic crystal-field component [the operator $\Delta H(\Gamma_2)$] induced by the isotopic disorder in the lattice destroys the equal spacing in the hyperfine structure. The energies of the hyperfine sublevels of the doublet Γ_{34} in the general case are equal to

$$E(\Gamma_{34})=E_c+\delta E+n_1\Delta E_1+n_2\Delta E_2\pm[(A_jm \times\langle+|J_z|+\rangle)^2+\langle+|\Delta H(\Gamma_2)|-\rangle^2]^{1/2}, \tag{42}$$

where E_0 is the energy of the doublet in the crystal field of the lattice of homogeneous composition (^{7}LiYF$_4$), and δE and ΔE_i are the average values of δH and $\Delta H(\Gamma_1)$ in the given state. Neglecting the displacements of the centers of gravity of the multiplets upon isotopic substitution of ions of the matrix, we can represent the shifts of the components of the hyperfine structure by the differences of the expressions (42) for the final and initial levels of the transition. The contributions to the change of the line frequency ν_{fi} that arise from $\delta E_f-\delta E_i$, $\Delta E_{1f}-\Delta E_{1i}$, and $\Delta E_{2f}-\Delta E_{2i}$ will be denoted by $\delta\nu$, $\Delta\nu_1$, and $\Delta\nu_2$, respectively.

The relative intensities of the lines that form the structure of the hyperfine components change with change of the lithium isotopic composition (Fig. 3). The measured intensities of the lines in the isotopic structure of the hyperfine components of the absorption lines agree well with those calculated in accordance with (40), if the following relations between $\Delta\nu_1$ and $\Delta\nu_2$ are fulfilled: a) $\Delta\nu\simeq\Delta\nu_1\simeq\Delta\nu_2$ [the transitions $\Gamma_{34}^1(^5I_8)$–$\Gamma_2^1(^5I_7)$ and $\Gamma_2^1(^5I_8)$–$\Gamma_{34}^1(^5I_7)$], and b) $\Delta\nu\simeq\Delta\nu_1$, $\Delta\nu_2=0$ or $\Delta\nu\simeq\Delta\nu_2$, $\Delta\nu_1=0$ for the other transitions with a resolved isotopic structure.[31] In addition, high-precision measurements of the structure of the line of the $\Gamma_2^1(^5I_8)$–$\Gamma_2^1(^5I_7)$ transition have made it possible to detect a sharply pronounced structure corresponding to occupation of sites R_1 and R_2 by impurity lithium isotopes with shifts $\Delta\nu_1\simeq0.005$ cm^{-1} and $\Delta\nu_2\simeq0.026$ cm^{-1}. The lines with the greatest intensity in the isotopic structure correspond to the case of absence of impurity isotopes in the immediate neighborhood of an Ho^{3+} ion ($n_1=n_2=0$), and it is from the relative shift of these lines in the ^{6}Li$_{0.9}$^{7}Li$_{0.1}$YF$_4$ and ^{7}LiYF$_4$ crystals that the quantities $\delta\nu$ given in Table IX were determined. In those cases when the lines are broadened because of phonon relaxation, and the isotopic structure is not resolved,

TABLE X. Periods of the isotopic structure of the absorption lines from the levels $\Gamma_{34}^1(^5I_8)$ and $\Gamma_2^1(^5I_8)$.

Final state		Initial state		Experiment	calculation	
				$\Delta\nu$, 10^{-3} cm^{-1}	$\Delta\nu_1$, 10^{-3} cm^{-1}	$\Delta\nu_2$, 10^{-3} cm^{-1}
$^5I_7$	Γ_2^1	$^5I_8$	Γ_{34}^1	13 $(\Delta\nu_1 = \Delta\nu_2)$	16,2	17,7
			Γ_2^1	25; 5	21,6	19,6
	Γ_{34}^1		Γ_{34}^1	16	14,6	19,2
			Γ_2^1	15 $(\Delta\nu_1 = \Delta\nu_2)$	20,0	21,1
	Γ_1^1		Γ_{34}^1	25	17,2	23,5
	Γ_2^2		Γ_{34}^1	18	17,4	15,5
			Γ_2^1	30	22,8	17,4
	Γ_{34}^2		Γ_{34}^1	24	19,9	23,3
			Γ_2^1	33	24,3	25,2
$^5I_6$	Γ_2^1		Γ_{34}^1	14	23,7	23,3
	Γ_1^1		Γ_{34}^1	18	17,9	20,8
	Γ_{34}^1		Γ_{34}^1	23	16,4	22,1
	Γ_{34}^2		Γ_{34}^1	13	18,6	21,3
			Γ_2^1	15	24,0	23,3
	Γ_2^2		Γ_{34}^1	33	30,5	23,9
	Γ_1^2		Γ_{34}^1	10	19,4	18,8
	Γ_2^3		Γ_{34}^1	24	26,9	21,6
$^5I_5$	Γ_{34}^1		Γ_2^1	34	27,9	23,8
$^5I_4$	Γ_1^1		Γ_{34}^1	< 18*	−0,3	14,9

Note: *The isotopic structure cannot be seen within the line width, and the value given is the latter.

we took for $\delta\nu$ the shift of the maximum of the line (which leads to an underestimate of $\delta\nu$). The calculated quantities $\delta\nu$ (the parameters δB_p^k from Table VII were used) are determined principally by the displacements of the initial levels of the transition. Upon substitution of ^{7}Li by the light isotope ^{6}Li the crystal field at the holmium ions becomes stronger, and the lower sublevels of the multiplets are shifted downward on the energy scale [in particular, $\Delta E[\Gamma_{34}^1(^5I_8)] = -0.104$ cm^{-1} and $\Delta E[\Gamma_2^1(^5I_8)] = -0.157$ cm^{-1}], and, since the total Stark splitting is a maximum in the ground multiplet $^5I_8$, the lines of centers with a light lithium isotope in the immediate neighborhood are always displaced in the direction of higher frequencies. As can be seen from Table IX, the results of the calculation are in satisfactory agreement with the measurements (when comparing the measured and calculated quantities $\delta\nu$ in Table IX the results of the calculations should be multiplied by 0.9, if we assume that $\delta\nu \sim x$). The average of the difference of the measured shifts of the two lowest sublevels of the ground multiplet is equal to 0.036 ± 0.005 cm^{-1}, and the calculated value of this difference is 0.048 cm^{-1}.

In Table X the measured intervals $\Delta\nu$ in the isotopic structure are compared with the results of calculations based on the estimates obtained above for the local deformation of $(\mathrm{LiF_4})^{3-}$ complexes containing the impurity lithium isotope. The directions of the shifts of the lines of the hyperfine structure in the case of successive occupation of the lithium sites near the Ho^{3+} ion by the light isotope ^{6}Li are determined uniquely by the displacements of the sublevels Γ_{34}^1 and Γ_2^1 of the ground multiplet in the crystal field specified by the operator $\Delta H(\Gamma_1)$. Some of the calculated possible periods of the structure differ from the measured ones by a factor of almost two, and the most important discrepancy between the data from the measurements and from the calculation performed is that the latter does not confirm the conclusion (which follows from an analysis of the relative intensities of the components of the isotopic structure) that there is a strong difference between $\Delta\nu_1$ and $\Delta\nu_2$ for most of the periods. Possible reasons for the quantitative discrepancy of the calculation results and the experimental data are: errors in the wave functions of the Stark sublevels (in particular, the deviation of the calculated expectation values of J_z in the sublevels of Γ_{34} from the values corresponding to the intervals of the hyperfine structure reaches 30%), errors in the estimate of the parameters of the local structure, and neglect of the displacements of the next-to-nearest neighbors of the impurity lithium isotope (a calculation performed by us in the framework of the quasimolecular model of an impurity center showed, in particular, that the displacements of the eight holmium ions near the impurity lithium isotope can reach 0.06×10^{-3} Å).

In accordance with (42), the rhombic component of the crystal field induced by the impurity isotopes of lithium exerts the strongest influence on the position of the hyperfine sublevels (of the Γ_{34} doublets) that correspond to the smallest values $m = \pm 1/2$ of the component of the nuclear angular momentum. In modulus, the calculated (using the data of Table VIII) matrix elements of the operators $\Delta H_i(\Gamma_2)$ on the wave functions of the doublets with a resolved isotopic structure do not exceed 0.022 cm^{-1}. According to the results of calculation, the rhombic component of the field is practically not manifested in the structure of the hyperfine sublevels of the ground state $\Gamma^1_{34}(^5I_8)$, but for a number of excited states the presence of different isotopes of lithium in the immediate neighborhood of the holmium ions leads to noticeably unequal spacing of the components of the hyperfine structure. In particular, in the doublet $\Gamma^1_{34}(^5I_7)$ the interval between the central components of the hyperfine structure in the case when one impurity isotope is present at the position R_1 is greater than the corresponding interval in a matrix of homogeneous composition by 0.008 cm^{-1}, which is in good agreement with the experimental estimate 0.01 cm^{-1} for this difference from the sharply pronounced unequal spacing of the isotopic structure of the transition $\Gamma^1_2(^5I_8)-\Gamma^1_{34}(^5I_7)$ (see Fig. 3). The rhombic component of the crystal field leads also to appreciable broadening of the lines of the isotopic structure as a consequence of the superposition of absorption lines of centers with different isotopic surroundings.

In conclusion, we note that the parameters obtained in this work for the crystal field induced by the inhomogeneous isotopic composition of the $\mathrm{LiYF_4}$ lattice can also be used to analyze the isotopic structure of the spectra of other rare-earth ions besides holmium. In Ref. 32 the observation of isotopic structure with intervals 1.4 GHz and width 0.6 GHz in the spectrum of an $\mathrm{LiYF_4{:}Er^{3+}}$ crystal with the natural content of lithium isotopes was reported; using the data of Table VII we have obtained shifts of the ground state of the $\mathrm{Er^{3+}}$ ion equal to $\Delta E(R_1) = -1.44$ GHz and $\Delta E(R_2) = -0.75$ GHz.

[1)] Preliminary investigations of the Raman light-scattering spectra have shown that an isotope effect can be detected.

[2)] The crystals were grown by M. A. Petrova and V. Yu. Egorov in the laboratory of A. I. Ryskin at the State Optical Institute, and the authors are grateful to them.

---

[1] N. I. Agladze, M. N. Popova, G. N. Zhizhin, V. J. Egorov, and M. A. Petrova, Phys. Rev. Lett. **66**, 477 (1991).

[2] G. F. Imbusch, W. M. Yen, A. L. Schawlow, G. E. Devlin, and J. P. Remeika, Phys. Rev. **136**, A481 (1964).

[3] C.-Y. Huang, Phys. Rev. **168**, 334 (1968).

[4] A. Hoffmann and U. Scherz, J. Cryst. Growth **101**, 385 (1990).

[5] N. Pelletier-Allard and R. Pelletier, J. Phys. C **17**, 2129 (1984).

[6] M. H. Nazare, A. J. Neves, and G. Davies, Phys. Rev. B **43**, 14196 (1991).

[7] K. W. Sandusky, J. B. Page, A. Rosenberg, and A. J. Sievers, Phys. Rev. B **47**, 5731 (1993).

[8] S. C. Lawson, G. Davies, A. T. Collins, and A. Mainwood, J. Phys.: Condens. Matter **4**, 3439 (1992).

[9] L. Canham, G. Davies, and E. C. Lightowlers, J. Phys. C **13**, L757 (1980).

[10] R. C. Buschert, A. E. Merlini, S. Pace, S. Rodriguez, and M. H. Grimsditch, Phys. Rev. B **38**, 5219 (1988).

[11] H. Holloway, K. C. Hass, M. A. Tamor, T. R. Anthony, and W. F. Banholzer, Phys. Rev. B **44**, 7123 (1991).

[12] B. Z. Malkin, in *Spectroscopy of Solids Containing Rare-Earth Ions* (North-Holland, Amsterdam, 1987), p. 13.

[13] A. K. Kupchikov, B. Z. Malkin, A. L. Natadze, and A. I. Ryskin, Fiz. Tverd. Tela **29**, 3335 (1987) [Sov. Phys. Solid State **29**, 1913 (1987)].

[14] S. A. Miller, H. E. Rast, and H. H. Caspers, J. Chem. Phys. **52**, 4172 (1970).

[15] H. H. Caspers and H. E. Rast, J. Lumin. **10**, 347 (1975).

[16] Vishwamittar and S. P. Puri, J. Phys. C **7**, 1337 (1974).

[17] P. Blanchfield, Tu Hailing, A. J. Miller, G. A. Saunders, and B. Chapman, J. Phys. C **16**, 3851 (1983).

[18] F. L. Aukhadeev, R. Sh. Zhdanov, M. A. Teplov, and D. N. Terpilovskiĭ, in *Paramagnetic Resonance*, No. 19 [in Russian] (Izd. Kazansk. Univ., Kazan, 1983), p. 3.

[19] L. A. Bumagina, V. I. Krotov, B. Z. Malkin, and A. Kh. Khazanov, Zh. Eksp. Teor. Fiz. **80**, 1543 (1981) [Sov. Phys. JETP **53**, 792 (1981)].

[20] A. K. Kupchikov, B. Z. Malkin, D. A. Rzaev, and A. I. Ryskin, Fiz. Tverd. Tela **24**, 2373 (1982) [Sov. Phys. Solid State **24**, 1348 (1982)].

[21] A. K. Kupchikov, B. Z. Malkin, A. L. Natadze, and A. I. Ryskin, in *Spectroscopy of Crystals* [in Russian] (Nauka, Leningrad, 1989), p. 85.

[22] J. Als-Nielson, L. M. Holmes, F. K. Larsen, and H. J. Guggenheim, Phys. Rev. B **12**, 191 (1975).

[23] P. Blanchfield and G. A. Saunders, J. Phys. C **12**, 4673 (1979).

[24] S. A. Al'tshuler and B. M. Kozyrev, *Electron Paramagnetic Resonance* [in Russian] (Nauka, Moscow, 1972).

[25] K. Rajnak and W. F. Krupke, J. Chem. Phys. **46**, 3532 (1967).

[26] H. P. Christensen, Phys. Rev. B **19**, 6573 (1979).

[27] N. Karayianis, D. E. Wortman, and H. P. Jenssen, J. Phys. Chem. Solids **37**, 675 (1978).

[28] A. V. Vinokurov, S. L. Korableva, B. Z. Malkin, A. I. Pominov, and A. L. Stolov, Fiz. Tverd. Tela **30**, 801 (1988) [Sov. Phys. Solid State **30**, 459 (1988)].

[29] N. I. Agladze and M. N. Popova, Solid State Commun. **55**, 1097 (1985).

[30] B. Pourat, B. Pilawa, and H. G. Kahle, J. Phys.: Condens. Matter **3**, 6069 (1991).

[31] N. I. Agladze, M. Beccucci, S. Califano, M. Inguscio, F. S. Pavone, M. N. Popova, and G. N. Zhizhin, Zh. Eksp. Teor. Fiz. **103**, 2215 (1993) [JETP **76**, 1110 (1993)].

[32] R. M. Macfarlane, A. Cassanho, and R. S. Meltzer, Phys. Rev. Lett. **69**, 542 (1992).

Translated by P. J. Shepherd